

UNIVERSITY OF ILLINOIS AT URBANA-CHAMPIAGN

ME 470: SENIOR DESIGN

Pool Evaporation

Final Design Report

Dec 11, 2020

Authors:

Authors: (Sorted Alphabetically)

Rodrigo Barreto	barreto3@illinois.edu	1 (312)-532-5134
Mitchell Hunter	mbh2@illinois.edu	1 (708)-941-6561
Kevin Liu	kevindl2@illinois.edu	1 (847)-907-1284
Juyi Zhang	juyiz2@illinois.edu	1 (217)-722-0656

Faculty Advisor:

Prof. Quinn M Brewster

TA:

Aakash Eetikala

Submitted To:

Vijay Sehgal
Sargent & Lundy
55 East Monroe Street
Chicago, IL 60603-5780

Contents

1	Executive Summary	1
2	Introduction	2
2.1	Spent Fuel Pools	2
2.2	Problem Statement	3
2.3	Literature Review	3
2.3.1	Empirical Models and Experimental Procedures	3
2.3.2	Numerical Simulation (CFD)	6
2.3.3	Analytical Models	6
2.4	Project Constraints	9
3	Experimental Design	9
3.1	Experimental Procedure	11
3.2	Siphon-Pan Mechanism	13
3.3	Heater	15
3.4	Standards	15
3.5	Experiment Data	16
4	Analytical Model	18
5	Budget	25
6	Conclusions and Recommendations	26
A	Matlab Code for Analytical Model	28
B	DAQ Arduino Code	29
References		33

List of Figures

1	Spent fuel pool	2
2	Dr. Pauken's apparatus for measuring evaporation rate of water	5
3	Comparing evaporation models	8
4	Dr. Raimundo's apparatus for measuring evaporation rate of water	10
5	Experimental Apparatus and Variables of Experiment	11
6	Tank and heater setup in the wind tunnel	12
7	Experimental Setup in the wind tunnel	13
8	Siphon-Pan Mechanism with the Heater	14

9	Evaporation Rate vs. Temperature	16
10	Evaporation Rate vs. Air Flow Rate	17
11	Diagram illustrating the theory of the Spalding Model	18
12	Comparison between Force Convection Data, CFD Simluation and Analytical Model Prediction	22
13	Comparison between Natural Convection Data and Analytical Model Pre-diction	23
14	Comparison between Our 1.75" Drop Data and Analytical Model Prediction	24
15	Comparison between Our Natural Convection Data and Boelter's Data . . .	25

List of Tables

1	Variable in the experiment	11
2	Budget	26

1 Executive Summary

Accurate models of evaporation of water in spent fuel pools are critical to ensuring safe disposal of nuclear fuel. However, compared to other bodies of water or liquids, such as indoor and outdoor swimming pools, there is comparatively little literature specifically modeling evaporation in spent fuel pools. While spent fuel pools are similar to other bodies of water, they are unique, because they contain radioactively decaying fission products, such as Uranium-235 and Plutonium-239, that provide a constant heat source that will boil the water without a proper cooling system.

The primary goal for the Fall 2020 semester was to both derive a model for the evaporation of water from spent fuel pools, and to compare said model to experimental results.

Accordingly, an experimental design is proposed below, as well as the finalized budget for conducting said experiment. A water tank was filled and placed within a wind tunnel, which was set to a constant air flow rate. A set of devices measuring air temperature, water temperature, humidity and the mass of the water in the tank were connected to a microcontroller, which output data to a text file. Experimental data was collected in this manner to describe how the rate of evaporation is affected by air temperature, water temperature, and humidity.

In addition to experimental work, Sargent and Lundy also desired a theoretical method of predicting evaporation rates for different configurations. Currently, Sargent and Lundy models the evaporation of spent fuel pools using the built-in Volume-of-Fluid CFD model in the Star-CCM+ software. Said simulation reportedly can take up to a month to run, due to the simulation accounting for the effects of phase change during evaporation. In response to the failures of the CFD modeling approach, the Spalding stagnant-film model of evaporation was paired with a correction factor, derived from curve-fitting the Spalding model to an evaporation dataset produced by previous research, to form an analytical model.

The evaporation rates produced by the resulting analytical model for each data point in the dataset used to derive the correction factor corresponded strongly to the evaporation rates listed in the aforementioned dataset, as well as the evaporation rates listed for each data point produced during this project.

2 Introduction

2.1 Spent Fuel Pools

Spent fuel pools are essential to the nuclear power industry. When nuclear fuel rods are no longer usable, they are stored in deep pools of water, as seen in Fig. 1, for years to cool them and allow remaining unstable isotopes, such as Uranium-235 and Plutonium-239, to decay. After this time, they are moved into dry cask storage where they will remain indefinitely. The large depth of water covering the fuel rods shields the nearby environment from radiation. Should the water level drop too low and place the spent fuel rods in danger of being uncovered, nuclear radiation will leak out of the pool into the surrounding environment.



Figure 1. Spent fuel pool

2.2 Problem Statement

Despite the importance of modeling evaporation in spent fuel pools, reliable empirical correlations specifically designed to model spent fuel pool evaporation are rare. This rarity is especially concerning due to the presence of a constant source of heat within the pool. In addition, the stringent set of regulations and review required of a model for it to be implemented within a spent-fuel pool cooling system restrict the use of models purely derived through curve fits to existing data. In addition, existing CFD models tested by Sargent and Lundy can often run for up to a month without delivering useful results. Therefore the main objective of this project is to derive an analytical model quickly and accurately determine the rate of evaporation of a spent fuel pool, with respect to variation in water temperature, air temperature, vapor pressure difference, and air speed, especially with respect to the difference in evaporation rate between natural convection conditions, where no airflow is forced over the water via fan, and forced convection conditions, where fans are used to force airflow over the water.

2.3 Literature Review

In order to derive the aforementioned model, several reports on the topic of spent fuel evaporation were reviewed and summarized below. Several different correlations between the rate of evaporation and various other factors were found in the literature. The papers are arranged with the model they are based on.

2.3.1 Empirical Models and Experimental Procedures

Empirical model

$$\dot{m}'' = C(p_w - p_a)^k$$

In the above formula, \dot{m}'' is the mass flux, while C and k are functions of flow speed. $p_w - p_a$ is the vapor pressure deficit.

The above empirical equation describes a series of empirical correlations widely used by different researchers to describe evaporation under forced convection conditions. Despite the popularity of these models, and the large size of the datasets said models are based on, these models, due to their nature as empirical correlations, lack generality, and are thus

excluded from our consideration for appropriate analytical models.

Michael T. Pauken. "An experimental investigation of combined turbulent free and forced evaporation", Experimental Thermal and Fluid Science, Volume 18, Issue 4, 1998, Pages 334-340

Formula: $\dot{m}'' = C(p_w - p_a)^k$ where $C = 74.0 + 97.97V + 24.91V^2$ and $k = 1.22 - 0.19V + 0.038V^2$

The above article outlines an empirical correlation in the form of $\dot{m}'' = C(p_w - p_a)^k$. In addition to formulating an empirical correlation, Pauken has provided an experimental setup developed in his earlier paper, *Novel method for measuring water evaporation into still air*. In order to measure the evaporation of water, Dr. Pauken proposed and utilized the apparatus [1] shown in Figure 2. An insulated, cylindrical water tank is placed under a wind tunnel. The wind tunnel uses draw-through fans to pull air across and parallel to the water. The rate of evaporation is measured by a digital scale, upon which is placed a pan of water, connected to the insulated, cylindrical water tank by a siphon. The decrease in mass measured by the scale is directly proportional to the amount of water evaporated inside the cylindrical water tank. This design was used as the initial template for the design used to collect physical data. The use of a siphon and auxiliary water pan allows for the use of relatively small scales to measure the change in mass of water in relatively large tanks. In the Pauken experiments, the maximum water temperature was 50°C and the maximum air flow velocity was 1.5m/s. Thus, the experiments conducted this semester aimed to expand these ranges into higher values, with a maximum water temperature of 90°C and maximum air flow velocity of 3 m/s. [1].

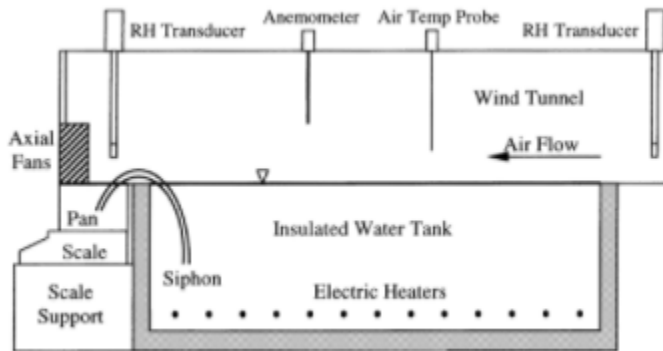


Figure 2. Dr. Pauken's apparatus for measuring evaporation rate of water

Charles Smith et al. "Measurement And Analysis Of Evaporation From An Inactive Outdoor Swimming Pool", Solar Energy, Volume 53, Issue 1, 1994, Pages 3-7

Formula: $\dot{m}'' = \frac{C(p_w - p_a)}{\Delta H}$ where $C = 30.6 + 32.1V$ and ΔH is the latent heat

In this paper, Dr. Smith has utilized experimental data to fit a model of evaporation based on that from ASHRAE Handbooks (1991). The relationship is measured in a pool with a water temperature of 29 °C, air temperature of 14.4 - 27.8 °C, and relative humidity of 27-65%[2]. The temperature range that the article covers is smaller than the operating range that our sponsor provides, but it offers a relationship in a certain region that can verify the validity of the constructed model.

L. M. K. Boelter et al. "Free Evaporation into Air of Water from a Free Horizontal Quiet Surface", Industrial Engineering Chemistry 1946 38 (6), 596-600

Formula: $\dot{m}'' = 251(C_{vw} - C_{v\infty})^{1.25}$ lb./(hr.)(sq. ft.)

In this paper, Dr. Boelter has shown another experimental setup he used to measure the natural convection evaporation rate. The resulting curves and equations cover the evaporation of distilled water from a 30.48-cm-diameter surface, within the temperature limit 17.2°C and 93.3°C, into quiet air at 18.3°C to 26.7°C and 54 to 98% relative humidity. Even though we did not adopt the physical setup, his data was extremely helpful when developing our analytical model. With the abundance of experimental data, we were able to construct an accurate analytical model.

2.3.2 Numerical Simulation (CFD)

Antonio M. Raimundo et al. "Wind tunnel measurements and numerical simulations of water evaporation in forced convection airflow", International Journal of Thermal Sciences, Volume 86, 2014, Pages 28-40,

In the paper, Dr. Raimundo conducted an experiment on pool evaporation and successfully established a CFD simulation. The experimental results are available in the paper and can be used to verify both the established model and the result of our own experiment. The experiment setup is also a good reference for our own design. However, it is worth noting that his experiment uses a relatively small tank, which can result in insufficient movement of the water surface. The simulation from the paper indicates that the CFD analysis is an applicable way to simulate the result. However, in the paper, Dr. Raimundo has used a modified turbulence Schmidt number for the specific experiment [3], and such modification may not be effective for other experiments. He has also noticed that the air velocity profile is changed when the water pool is presented. Such an effect might indicate a horizontal movement of the water and such movement might have an effect on evaporation. Additionally, Dr. Raimundo has compared the result of different empirical model with his experiment and CFD Simulation. He concluded that the numerical and the experimental results are very close, while empirical model tends to overestimate or underestimate the result, and the region where the empirical model holds accurate are only valid for a small range. The discussion has inspired us to choose the more challenging analytical model as our study model and the model we researched on is discussed below.

2.3.3 Analytical Models

Other than the empirical model researched above, there are also other models that take on a theoretical approach. These models are more fundamental with primitive input and independent variables based on fundamental formula. It is more based on theory compared to the empirical correlation but also has an empirical fitting to ensure the accuracy. However, it is worth noting that many of the analytical models are focusing on natural convection while the discussion of forced convection is not as much as that for natural convection. The forced convection brings several more parameters to the model and is more difficult to predict due to turbulence (Generally, a lower Reynolds number, indicating laminar flow, can be predicted from solving species equation since the gradient converges. However, in turbulent flow with high Reynolds number, the prediction become difficult and will rely on

empirical relationship of different dimensionless groups.

B. R. Hugo et al. “Evaluation of the fukushima daiichi unit 4 spent fuel pool,” International Nuclear Safety Journal, vol. 4, no. 2, pp. 1–5, 2015

$$\text{Hugo's Model: } \dot{m}''_{Hugo} = 9.24(1 + 2v^{1.35})^{0.67} \frac{T}{273} \ln \frac{P - P_{1,e}}{P - P_{1,s}} [4]$$

In the paper, Dr. Hugo has offered the diffusion model of evaporation and used different model to predict the behavior of Fukushima Daiichi Unit 4 Spent Fuel Pool. Additionally, he has provided his understanding of the Shah's model and compared the performance of different models in predicting evaporation. The Hugo Model is a straightforward model. However, due to accuracy, we have chose to adopt the Spalding model.

M. Shah, “Methods for calculation of evaporation from swimming pools and other water surfaces,” ASHRAE Transactions, vol. 120, pp. 3–17, 01 2014.

$$\text{Shah's Model: } \dot{m}'' = 35\rho_w(\rho_r - \rho_w)^{1/3}(W_w - W_r) \text{ or } \dot{m}'' = 5 \cdot 10^{-5} \left(\frac{v}{0.15}\right)^0.7 * (P_w - P_r) [5]$$

In the paper, Shah has derived his formula for evaporation by natural convection. She has also considered different boundary conditions and utilized different formulas. Her concentration in the paper did not specifically focus on spent fuel pools, and the instructions for using the model are complex.

However, the ability to combine a theoretical model with empirical curve-fits offered by the correction factor within the Spalding model empowering it with a great degree of flexibility. In addition, in Figure 6 of Dr. Brewster's paper, ”Evaporation of water at high mass-transfer rates by natural convection air flow with application to spent-fuel pools,” it is clear that, compared to the Spalding model, the Hugo and Shah model tends towards underestimating evaporation rates. Since underestimating the evaporation rate is more dangerous than overestimating it, the Spalding model was selected for further development.

M. Quinn Brewster, Evaporation of water at high mass-transfer rates by natural convection air flow with application to spent-fuel pools, International Journal of Heat and Mass Transfer, 2017

Spalding Model: $\dot{m}'' = g_m B_m$ where $B_m = \frac{m_{1,s} - m_{1,e}}{1 - m_{1,s}}$ and $g_m = \frac{-\rho D_{12}}{m_{1,s} - m_{1,e}} \frac{\partial m_1}{\partial y}|_s$ where g_m can be obtained from g_m^* multiplied by $\frac{g_m}{g_m^*}$

In this paper, Professor Brewster has derived a numerical solution for mass flux using the Spalding model. He has also discussed different models of evaporation, and has con-

cluded that the Spalding model corresponds well with the data collected [6]. Therefore, we have decided that the model should be used as our primary model to study. However, the paper is mostly researching natural convection, and the effect of forced convection still needs to be studied.

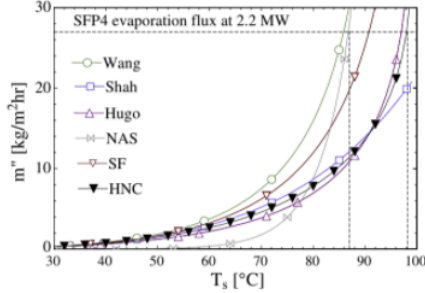


Fig. 6. Comparison of various model predictions of quasi-steady pool temperature and evaporative mass flux for decay heat of Fukushima SFP4 within days after station blackout for $T_e = 20^\circ\text{C}$, $\text{RH}_e = 50\%$, $Sc = 0.62$, and $Pr = 0.70$.

Figure 3. Comparing evaporation models

Bergman, T. L. , Lavine, A. S. , Incropera, F. P. , and DeWitt, D. P. , 2011, *Fundamentals of Heat and Mass Transfer*, 7th ed., Wiley, New York

In the textbook "Fundamentals of Heat and Mass Transfer," an example is given for forced convection in a swimming pool that we used as one of the basis of our forced convection corrections to the Spalding model. In the example, Bergman finds the Reynolds number at the trailing edge of the pool $U_\infty L/v$, and when combined with the Schmidt number, a Sherwood number correlation for forced convection is obtained $S\bar{h}_L = 0.037 * Re^{4/5} * Sc^{1/3}$. Combining this with the density of saturated water vapor and the diffusion coefficient for water, he calculated the evaporation rate $n_A = \bar{h}_m A (\rho_{A,s} - \rho_{A,\infty})$. The example pointed out the relationship between the Sherwood number in forced convection and the Reynolds number and the Schmidt number, and is helpful in transforming a relationship with velocity to a relationship with different dimensionless groups.

In conclusion, with the literature review, we have decided to design our experiment based on Dr. Raimundo's setup while referring to Dr. Pauken's weight measurement apparatus. For the analytical model we have chosen the Spalding model as our primary research model with certain modifications on forced convection, and the result will be discussed later in the Analytical Model Section.

2.4 Project Constraints

To achieve the goals outlined in the problem statement, the following tasks must be completed:

- Derive an analytical model from existing literature on water evaporation
- Compare with competing models
- Perform an experiment to verify and evaluate the performance of the model
- Further verify analytical model with CFD model

Note that the sponsor's previous attempts to replicate Pauken's experiment with a CFD model did not converge after a month of runtime. Further attempts at CFD may face similar issues, preventing delivery of a CFD model.

3 Experimental Design

One objective of the semester was to create an experimental design that could run tests and produce real data to be analyzed. The data collected could be compared with existing data from the Boelter and Raimundo experiments. If the data collected showed similar trends to the published experiments, it would verify that the design created was producing valid results that could be used in an analytical model. After reading about experimental setups in the literature review, the control parameters and variables were defined for the physical model.

A testing environment in which the air temperature and humidity could be controlled was needed. The water temperature and the air flow velocity also needed to be varied and recorded. The mass change in the tank needed to be measured over a specified time period to calculate the evaporation rate. Through university resources and help from Professor Brewster, the wind tunnel in the basement of Talbot Hall was made available. The wind tunnel created a controlled environment that could keep a consistent air temperature and humidity. The air flow velocity could also be varied inside of the wind tunnel. A water tank was needed to hold that water during the testing.

In Pauken's experimentation, a water tank was mounted to the bottom of the wind tunnel, but this method was not possible. The tank was placed inside of the tunnel, which changed the cross-sectional surface area in the tunnel and disrupted the laminar flow. Construction board was placed throughout the length of the wind tunnel to create a level surface. Because the volume in the tunnel was changed, the wind speed was measured manually using an anemometer.

The water in the tank needed to be heated to a temperature and then held at that temperature for the three hours that the test ran. Research was completed on water heaters, which lead to the discovery of the sous vide, a submersible induction heater that could safely and accurately heat up to five gallons of water to temperatures between 25-90°C. A five gallon tank with dimensions that could fit the constraints of the wind tunnel was purchased. The sous vide heater was also able to maintain the temperature of the tank and circulate the water to keep the temperature consistent throughout the tank. To verify the accuracy of the sous vide reading, four thermocouples were placed in different areas of the tank to measure the water temperature. The thermocouples were attached to an Arduino circuit that printed the data to a computer.

RH-transducers (AM2302) were also connected to the Arduino circuit to measure the air temperature and humidity. The scale used could only measure up to 12kg, but the tank filled with water exceeded this limit. A weight pan connected via a siphon was used, similar to the Pauken design. Evaporation of water from the larger tank would induce a proportional reduction of mass in the smaller pan placed upon a scale. The mass ratio was calculated so that the mass difference measured in the weight pan could be used to calculate the mass difference in the water tank. The scale was connected to the Arduino circuit so that the mass could be read throughout the experiment. Additionally, a camera was mounted above the tank, and floating particles were placed on the surface to observe any disturbance. The experimental setup can be seen in Fig. 5.

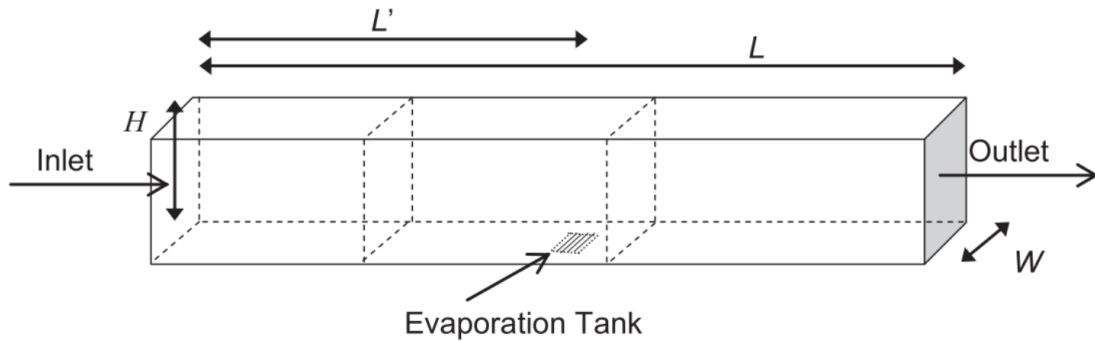


Figure 4. Dr. Raimundo's apparatus for measuring evaporation rate of water

3.1 Experimental Procedure

Table 1. Variable in the experiment

Variable	Symbol	Unit
Water Temperature	T_w	°C
Water Vapor Pressure	P_w	°C
Partial Pressure of water in Air	P_a	MPa
Flow speed	V	m/s
Distance between Water Surface And Top of Tank	d_{step}	m
Length of Water Tank	L	m
Evaporation rate or mass flux	J or m''	$g/(m^2 s)$

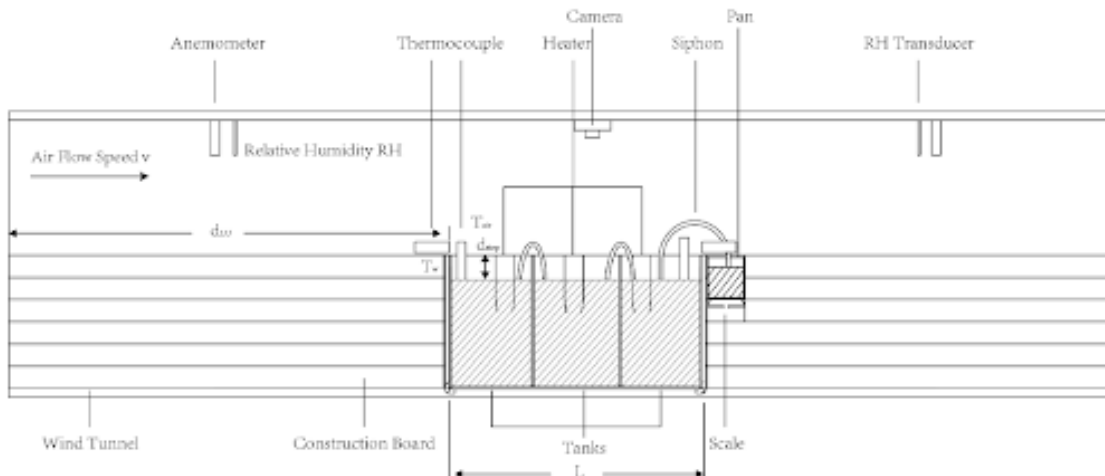


Figure 5. Experimental Apparatus and Variables of Experiment

Once the experiment was setup inside the wind tunnel with construction board guiding the airflow to the brim of the water tank, we had to attach the sous vide heaters to the edge of the tank and set it to the desired temperature. We conducted experiments in one and two tanks connected by a siphon as that was the most efficient way we found to vary the surface area of the tank. In the one tank experiments we used one sous vide heater since it can heat up to 5 gallons of water. After setting up the heater, we placed our Arduino circuit in the tank. The circuit consists of 4 copper/constantan T-thermocouples, 2 AM302 humidity sensors, and a scale, all those are connected to an Arduino Mega through a bread board circuit. The T-thermocouples are placed in different positions along the tank to ensure constant water temperature, the AM302 humidity sensors are positioned around the tank to measure the humidity inside the wind tunnel over time, and the scale is positioned under the pan-siphon mechanism to measure the weight variation over time. The data is collected through an Arduino code for further analysis.

Three water tanks were placed along the length of the tunnel, as shown in Fig. 5. The wind tunnel will be set to different wind flow speeds to observe the effects of convection on the surface of the pool. A run-up distance on evaporation is designed using construction boards to ensure the air flow is perpendicular to the brim of the tank. We will also change the water level to observe how a step between the surface of the water and the brim of the tank will affect evaporation. The image of the experimental setup is shown in Figure 6 and Figure 7

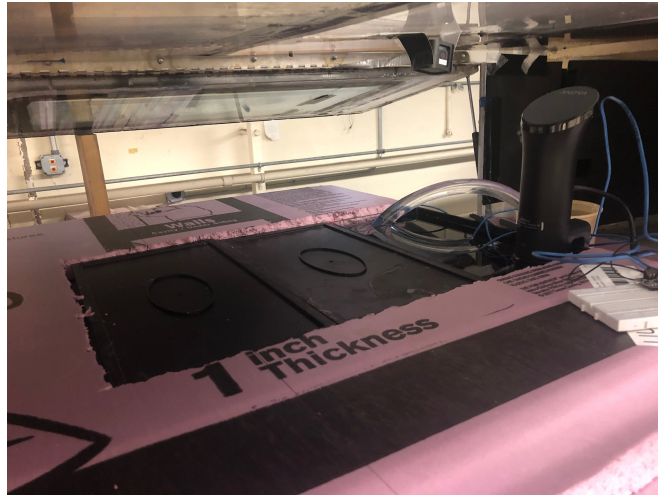


Figure 6. Tank and heater setup in the wind tunnel

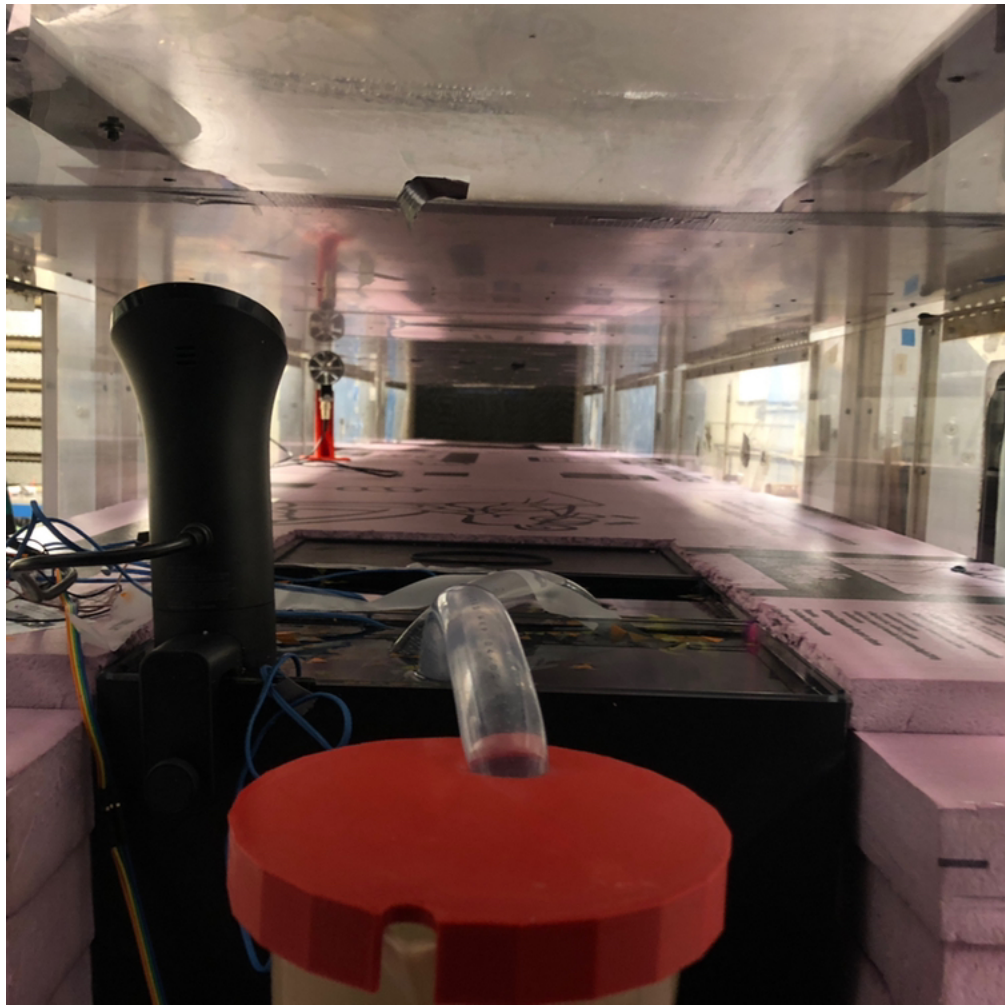


Figure 7. Experimental Setup in the wind tunnel

3.2 Siphon-Pan Mechanism

To measure the amount of water evaporated from the tank we used a siphon-pan mechanism based on Dr. Pauken's experiment and the setup is shown in Figure 8. The idea is that as the water evaporates in the main tank due to forced and natural convection the water will flow from the pan to the main tank and since we are monitoring the weight in the pan through the load cell connected to the Arduino we can figure out how much water evaporated in the tank over time.



Figure 8. Siphon-Pan Mechanism with the Heater

Some of the issues we came upon when using the mechanism were that we needed a cap for the pan, otherwise the natural and forced convection would affect it as well. Another issue was figuring out how the mechanism worked since in Pauken's paper there isn't an explanation of the mechanism. We figured out that initially the siphon connection between the tank and the pan makes both containers have the same level of water in them, and as water evaporates from the tank it is replaced due to pressure change. Overall, the siphon-pan mechanism was not the best for our experiment, ideally the water evaporated would be measured directly from the tank while finding a way to keep the water level constant.

3.3 Heater

To heat the tank to the desired experiment temperatures we chose Sous Vide heaters. Our choice was based on the fact that the cooking device is good for maintaining a constant water temperature in the desired range between 25 and 90 degrees Celsius that can translate to possible observable temperatures inside a spent fuel pool, the heater also has a immersed circulator mechanism that is able circulate the water inside the tank, which makes the temperature of the water uniform allover the tank while not disturbing the water surface.

Fully immersible heaters that produced a constant power input were also considered, however, those heaters showed an issue when controlling the temperature in the tank and keeping it constant. Also, fully immersible heaters did not have a mechanism to move the water, so the temperature in the locations where those heaters were located would be higher then its surroundings and that temperature variation within the tank would affect the overall experiment.

The sous vide heaters are 32.512cm tall with 5.6cm in diameter, the maximum power is 750W, which can heat up to 20 liters with a 0.1°C accuracy. Because the the sous vide is not completely immersed and works with a clamp to the edge of the tank with x cm sticking out of the water we had to attach the heater to the furthest edge of the tank so that it wouldn't affect the airflow and the area occupied by the heater had to be subtracted from the surface area of the water for all calculations.

3.4 Standards

The experiment was constructed taking into account the ASME Guidance Manual for Model Testing Part 23 (Instruments and Apparatus). According to the manual, "a model is a device machine, structure or system which can be used to predict the behaviour of an actual and similar device, machine, structure or system... a physical model can be smaller than, the same size as, or larger than the prototype". In those aspects our experiment fits the definition of a model according to the ASME. However, in further sections of the manual the concept of geometric similarity is introduced and since Sargent Lundy was not able to disclose the dimensions of the spent fuel pool in question we had to work with a distorted geometric model. Our experiment also fulfills the requirements for dynamic and kinematic similarity, where the forces acting and the motions in the fluids are the same in the model and the prototype.

Data was collected using common dimensions and units in accordance to the S.I. (Met-

ric) units as suggested by the ASME Council. The dimensionless variables calculated in our analytical model were approved by the ASME as shown in the Guidance Manual appendix.

3.5 Experiment Data

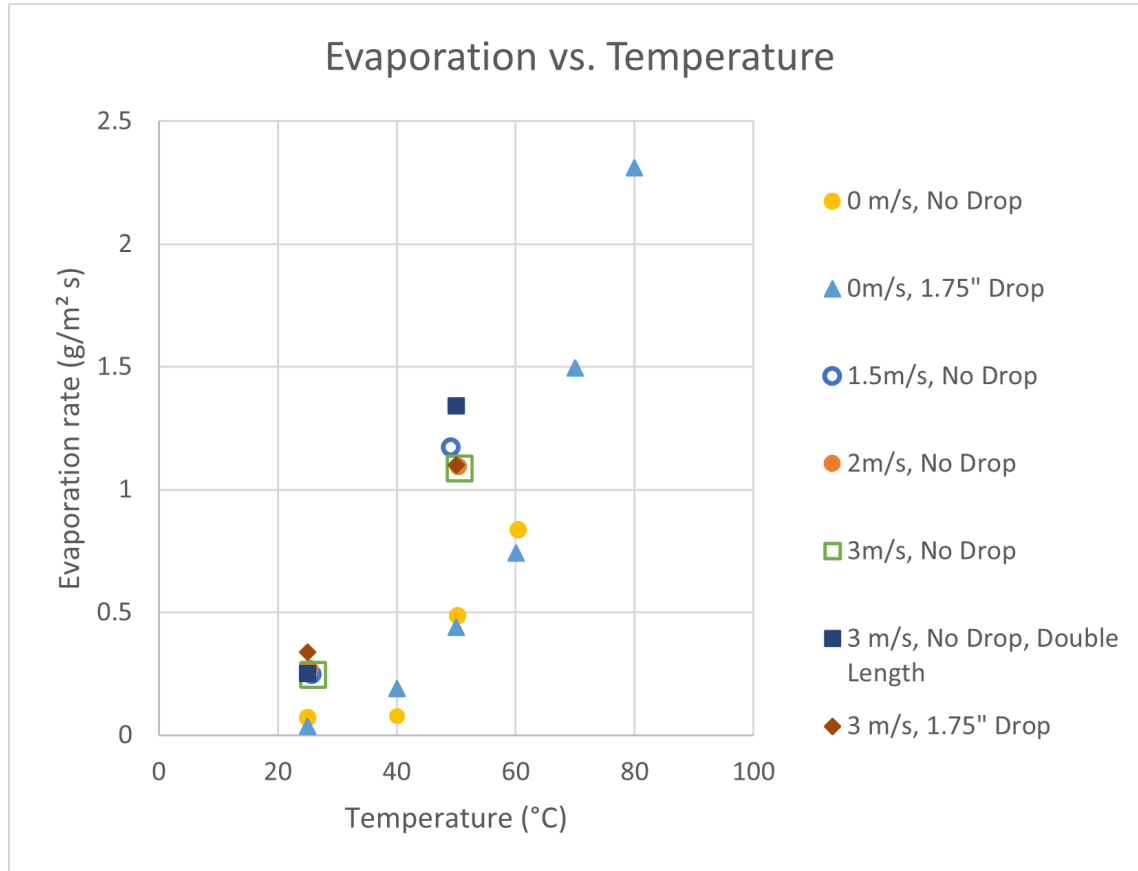


Figure 9. Evaporation Rate vs. Temperature

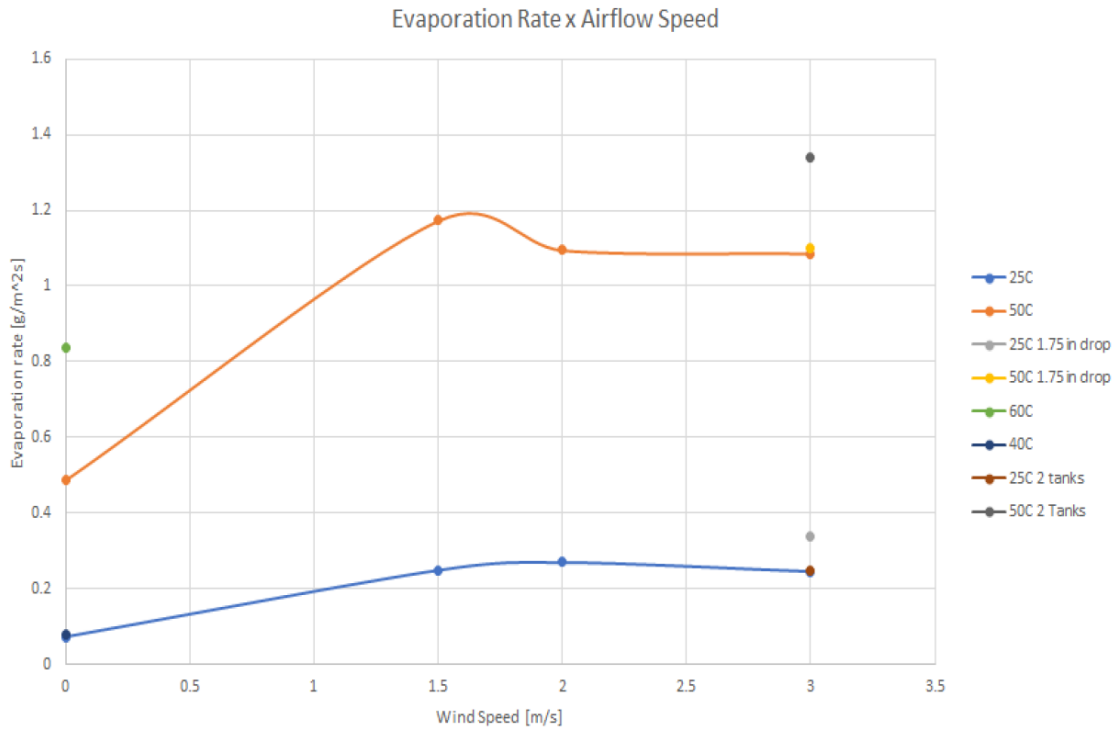


Figure 10. Evaporation Rate vs. Air Flow Rate

Increasing water temperature increases evaporation rate (Fig. 9). Shielding the water surface from the wind by lowering the height of the water does not seem to have an effect on evaporation rate, nor does increasing the length of the water tank, as seen by the small difference between series with the same wind speed (Fig. 9).

Increasing flow rate from 0 to 1 m/s increased evaporation rate, as expected (Fig. 10). However, increasing flow rate from 1.5 m/s to 3 m/s had little effect on evaporation. A possible explanation for these results lies in the humidity build up above the tank. In the free convection tests, as the water evaporated, the air above the tank became more humid, which made it harder for the water to continue evaporating. As a forced air flow was introduced, the humid air was pushed away from directly above the tank. The evaporation was then able to proceed at its initial rate. The evaporation rate was slow enough, that the lowest forced convection velocity tested was sufficient to clear the humid air buildup before it could effect the evaporation rate. Therefore, the higher velocities had the same effect, which led to the evaporation rates for each temperature to be the same at a 1.5m/s

air flow and at a 3m/s airflow.

The expectations for further testing are that under forced convection conditions, that length and distance of water surface from top of the tank will have no effect on evaporation, and that evaporation rate will increase with wind speed at low speeds, and will stay constant at high speeds. The air speed at which the evaporation rate levels off is expected to be higher for higher temperatures.

4 Analytical Model

The analytical model is constructed based on the Spalding model as we have discussed previously. The Spalding model is constructed based on the mass balance at interface shown in figure 11[7].

$$q_{c,u} + \dot{m}'' h_u = \dot{m}'' h_s + q_{r,s} + q_{c,s} + j_{i,s} h_{i,s} \quad (1)$$

$$\dot{m}'' = j_{1,s} + \dot{m}'' m_{1,s} = -\rho D_{12} \frac{\partial m_1}{\partial y}|_s + \dot{m}'' m_{1,s} \quad (2)$$

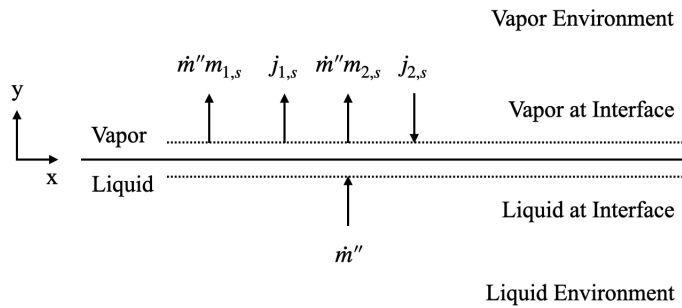


Figure 11. Diagram illustrating the theory of the Spalding Model

We can rearrange the relationship using the Spalding B-Number and the g-conductance, and the rearranged relationship is

$$m'' = g_m B_m \quad (3)$$

$$B_m = \frac{m_{1,s} - m_{1,e}}{1 - m_{1,s}} \quad (4)$$

$$g_m = \frac{-\rho D_{12}}{m_{1,s} - m_{1,e}} \frac{\partial m_1}{\partial y} \Big|_s \quad (5)$$

As we can see the relationship relies on solving species equation and can therefore be difficult to solve. The reason is that the equation depends on the gradient term. The term can be solved in some special types of flow like Laminar flow and the solution can be obtained in both low-blowing condition and higher blowing condition. However, there are also other types of flow that involves turbulence (for both natural convection and forced convection) and obtaining a solution for these conditions are complicated. Instead, we can utilize dimensionless group in our calculation.

From the previous work of Professor Brewster and other researchers, we are able to solve for a limited solution at lower evaporation rate to avoid directly solving the species equation. To solve for the limited solution, we use the Sherwood number for the mass flux and the Nusselt Number for the heat flux.

$$g_m^* = \frac{\rho D_{12}}{L} Sh \quad (6)$$

$$g_h^* = \frac{\rho \alpha}{L} Nu \quad (7)$$

The Sherwood number can be derived from mass Rayleigh number and the Nusselt number can be derived from Rayleigh number with the correlation shown below

$$Nu = 0.14 Ra_h^{1/3} \quad (8)$$

$$Sh = 0.14 Ra_m^{1/3} \quad (9)$$

The heat Rayleigh number and the mass Reyleigh number can be obtained from the heat/-mass Grashof Number, the Prandlt Number and the Schmidt Number

$$Ra_h = Gr_h \cdot Pr = \frac{g \beta (T_s - T_e) L^3}{\nu^2} \cdot \frac{\nu}{\alpha} \quad (10)$$

$$Ra_m = Gr \cdot Sc = \frac{g (\rho_s - \rho_e) L^3}{\rho \nu^2} \cdot \frac{\nu}{D_{12}} \quad (11)$$

Using the formula we are able to obtain the low evaporation rate solution. However, it is worth noting that no detailed flow information is contained in these correlation to obtain solution at higher evaporation rate, a correction term is used denoted as (g/g^*) . From the

data we obtained from Dr. Boelter and Dr. Raimundo, we are able to construct our own experimental model based on the Spalding model. We developed our correction factor as

$$\left(\frac{g}{g^*}\right)_{m,h} = \frac{0.09738 * T - 22.5756}{e^l} \frac{\ln(1 + B_{m,h})}{B_{m,h}} \quad (12)$$

It is worth noting that for the Spalding model, various correction factors are used in different conditions. However, it is worth noting that equation 12 will only hold true for the natural convection case. Combining with the literature from Theodore L. Bergman, we have managed to come up with a forced convection solution by modifying the Sherwood Number. We note the Sherwood Number from the natural convection case to be Sh_n , we then have the Sherwood Number from the forced convection only to be Sh_f , from dimensional analysis

$$Sh_f = f(Re, Sc) \quad (13)$$

$$Sh_f = C \cdot Re^a Sc^b \quad (14)$$

In the data we have found that linear relationship describes the velocity and the evaporation rate well, and the relationship we found is

$$\dot{m}'' = B \cdot g^* \cdot \frac{g}{g^*} + 0.156V \quad (15)$$

Since we know velocity u , characteristic length L (which is the length of the pool), and the kinematic viscosity of the air, we can calculate the Reynolds number

$$Re = \frac{uL}{\nu} \quad (16)$$

We have obtained the range of the Reynolds number to be 837-5776.2. From the empirical relationship between the Sherwood Number and the Reynolds number, we know the power of Reynolds number will be 0.5 for laminar boundary layer and 0.8 for turbulent boundary layer. Since the Reynolds number in the experiment are at the transition area, we are supposing that $a = 0.55$, which later has proven to fit the data well.

Since we know

$$Sc = \frac{\nu}{D} \quad (17)$$

and the Schmidt number are generally having a power of $1/3$ in different relationships. Therefore, we are using the same power in our relationship. We have then used our previous

relationship and found that $C = 0.542$, and the developed forced convection only Sherwood Number is

$$Sh_f = 0.38 \cdot Re^{0.55} Sc^{1/3} \quad (18)$$

We also have the relationship for the Nusselt number in forced convection

$$Nu = 0.332 Re_L^{1/2} Pr^{1/3} \quad (19)$$

where Pr is Prandlt Number defined as

$$Pr = \frac{\nu}{\alpha} \quad (20)$$

In the Prandlt Number ν is the momentum diffusivity and α is the thermal diffusivity Combined with the natural convection Sherwood Number, we now have the Sherwood number for mixed convection

$$Sh = Sh_n + Sh_f = 0.14(Gr \cdot Sc)^{1/3} + 0.38 \cdot Re^{0.55} \cdot Sc^{1/3} \quad (21)$$

We will continue to use the g-conductance and the Spalding B number as in the natural convection case whose formula is

$$g_m^* = \frac{\rho D_{12}}{L} Sh \quad (22)$$

$$g_h^* = \frac{\rho \alpha}{L} Nu \quad (23)$$

$$\dot{m}'' = g_{m,h}^* B_{m,h} \left(\frac{g}{g^*}\right)_m \quad (24)$$

$$\left(\frac{g}{g^*}\right)_{m,h} = \frac{\ln(1 + B_{m,h})}{B_{m,h} e^l} \quad (25)$$

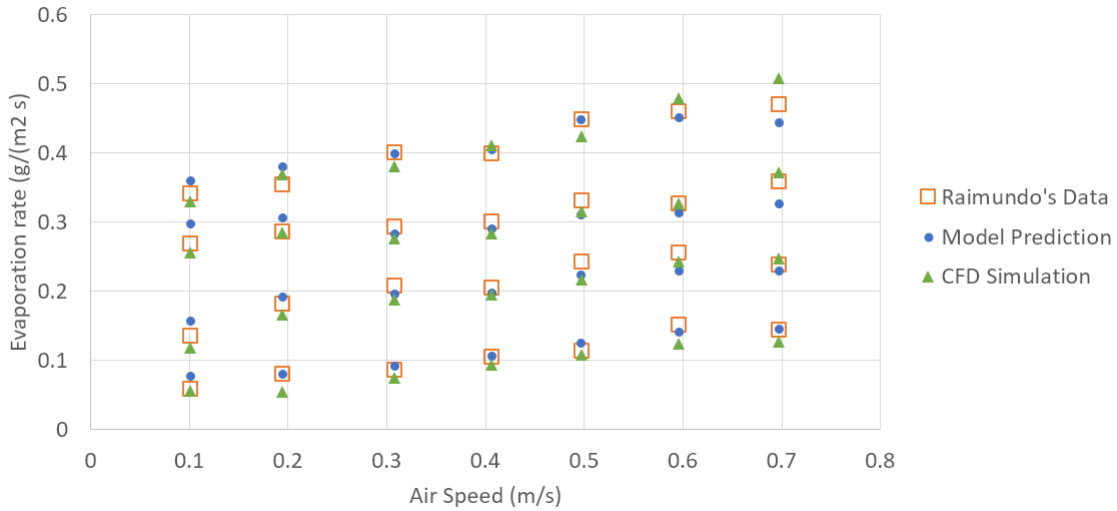


Figure 12. Comparison between Force Convection Data, CFD Simluation and Analytical Model Prediction

We can use this number to solve for the evaporation rate and we have utilized data from previous forced convection, natural convection, and our own experiment. The result of our analytical model compared to the forced convection data [3] is shown in Figure 12. We have also included the CFD Analysis from the same paper as a reference to the performance of our analytical model. As shown in the figure, our model has in fact matches or outperforms the accuracy of the CFD Model, our error percentage is below 10% and at many data point below 5%.

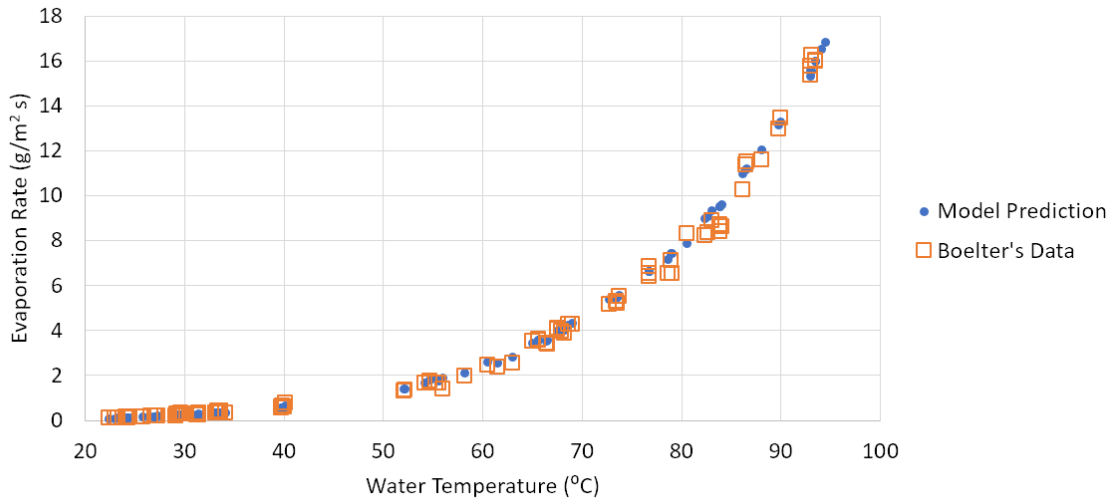


Figure 13. Comparison between Natural Convection Data and Analytical Model Prediction

In addition to the forced convection data, which studies a relatively smaller temperature range. We have also generated our prediction on natural convection experimental data from Dr. Boelter [8], and the result also matches well. The comparison is shown in Figure 13. As we can see from the figure, the experimental data and the model is matching extremely well, many of the predictions are overlapping with the experimental data and the accuracy is extremely high with an average accuracy of 5%

Professor Brewster has also provided a comparison between the same natural convection data and his model prediction. He is using a correction factor of $1/(1 + 1.5B^{0.8})$ and has resulted in a promising result.

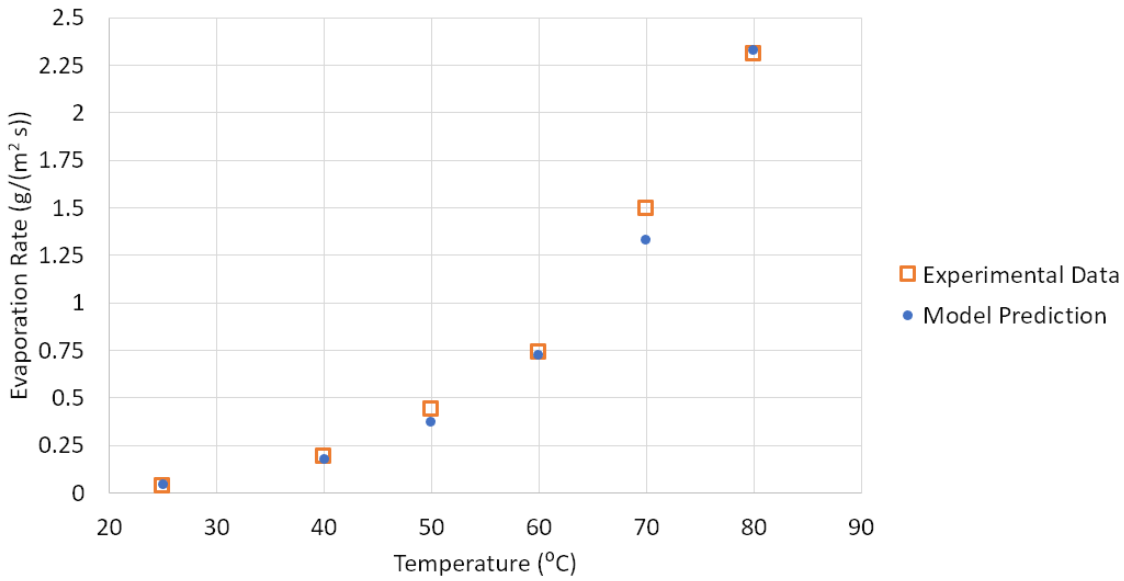


Figure 14. Comparison between Our 1.75" Drop Data and Analytical Model Prediction

Lastly, we have also utilized our experimental data and the comparison between the prediction and experimental data is shown below. We have not changed any of our parameters. However, the model worked out really well for the experimental data with a drop distance. Further confirming the accuracy and generality of our experimental Data. The comparison between our natural convection data at 1.75" Drop and the model prediction is shown in Fig 14. The prediction fits well with the experimental data without any additional fitting

However, it is worth noting that since other experimental data we have obtained is having significant error compared to the existing natural and forced convection data, as shown in figure 15. The error is possibly due to the inaccuracy of our siphon-pan measuring device. Therefore, We have not include these data in our analysis. For the forced convection In terms of the forced convection, there are some difficulties for the analytical model to predict. We are unable to obtain the evaporation data at lower flow speed due to equipment restriction, and for the data measured, the speed of 1.5m/s, 2m/s, and 3m/s are having an evaporation rate near each other, thus making the model's prediction difficult.

However, we have tried to interpolate the data for all cases and found that at the 1.5m/s, 298K case, the actual evaporation rate is still within the prediction of the model at 0.249 $g/(m^2 s)$ (the model prediction is 0.2909), but not for the 2m/s and 3m/s case. The 323K

case has a lower result than the prediction (for 1.5m/s, the experimental result is 1.17 while the model prediction is 1.389). We assume that the water level is becoming lower as the experiment continues and therefore the drop prevents the evaporation by an increased relative humidity inside the tank.

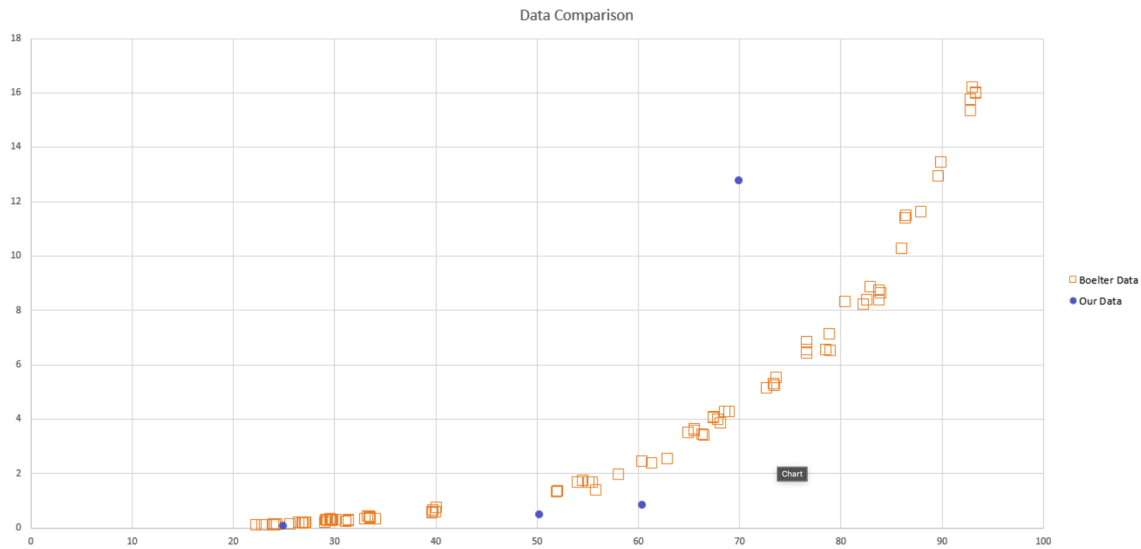


Figure 15. Comparison between Our Natural Convection Data and Boelter’s Data

5 Budget

The total budget of this project, provided by Sargent and Lundy to the MechSE department, is \$1500. The budget for our physical prototype can be seen in Table ???. Funding will be used to purchase materials required for implementing the experimental design. The rest of the project work is to be completed in a variety of applications that currently are available to UIUC students for no cost.

Our main cost for the project is building the experiment as the other deliverables requested by the company are done through softwares available to us by the university. The first design based on Dr. Pauken’s experiment would cost us around \$954.25, as you can see in the Bill of Materials below. This cost corresponds to a small part of the budget and we used existing laboratory facilities at the University of Illinois that already had some of the devices we need to create the apparatus and collect data. If that is the case we would

be able to make the cost even lower.

Table 2. Budget

Item	Unit Price \$/Unit	Quantity Unit	Total \$
Construction Board 2in	11.00	6	66.00
Construction Board 1in	19.98	1	19.98
Scale	11.99	1	11.99
Siphon	25.00	1	25.00
Pan	0.00	1	0.00
Sous Vide Heater	129.00	3	387.00
T-Type Thermocouple	0.00	4	0.00
Anemometer	0.00	1	0.00
AM2302 Humidity Sensor	15.00	2	30.00
Camera	0.00	1	0.00
Arduino Mega	40.30	1	40.30
MAX31856	17.50	4	70.00
Aquarium	49.99	3	149.97
Aquarium	40.00	1	40.00
Total Cost			\$954.25

The Bill of Materials corresponds to the list of equipment needed to build our experimental design.

6 Conclusions and Recommendations

The physical model was able to provide data that had similar trends to the results from Spalding and Raimundo, so tests were completed throughout the defined water temperature and air flow velocity ranges. The free convection data showed that as water temperature was increased, so was the evaporation rate. In the forced convection test, the evaporation rate increased as an air flow was presented. However, after the initial forced air flow was introduced, the evaporation showed no significant change as the air flow was increased. This meant that the initial air flow velocity was significant enough to clear out any humidity build up above the tank fast enough to maintain the evaporation rate.

An analytical model was developed from the literature reviewed and the physical data obtained. The analytical model was based on the Spalding model and work was done to investigate the correction factor for natural convection. Additionally, the forced convection Sherwood number was found and integrated into the analytical model. With the combination of an improved correction factor for the natural convection case and the introduction of a forced convection Sherwood number, high fidelity predictions were obtained that match the accuracy of a CFD Model. In comparison with the experimental results, the predicted data had a percentage error of 5%-10%.

If this project were to be done again, more time and access to resources would be recommended. The experimentation provided data that was insufficient to prove any correlations or trends, but it showed promising results for certain configurations. More time would allow for more tests to be run to further verify the validity of the data collected. The wind tunnel was a valuable resource, and more time with it would allow for more than one test to be ran at each data point. This would eliminate outliers and provide more accurate data. This project has potential to be further investigated in future semesters. The model provided results that did not agree with existing data for forced convection evaporation. This issue should be investigated before further testing. Further data collection with a modified model should be completed so that certain relationships could be factually proven and considered accurate in the spent fuel pool evaporation industry. As previously stated, there is no published data for pool evaporation under the higher temperatures and air flow velocities that were tested. Sargent and Lundy has also expressed interest in the development of a computational fluid dynamics analysis. Due to time constraints and a lack of experience in CFD software, this was not able to be completed within the semester. The physical and analytical models are still in the preliminary stages, but upon significant improvement and an extended time period of data collection, the data obtained should be turned over to students with superior fluid dynamics experience, ultimately leading towards the development of a CFD model for Sargent and Lundy.

A Matlab Code for Analytical Model

```
function evap = Revised_Code(Ta,Tw,Pw_minus_Pa,V,drop)
Pa = 1000000;
Pw = Pw_minus_Pa + Pa;
L = 1;
ABST = Tw;
ABSTA = Ta;
air_kin_viscosity = 1.81*10^-5;
Re = V*L/air_kin_viscosity;
D12 = 4.14*exp(0.0061*ABST)*10^-6; % T is in terms of Kelvin, coefficient
in terms of m^2/s
P1 = Pw;
P1e = Pa;
M2 = 29;
M1 = 18;
m1 = P1/(Pw*(M2/M1)-P1*(1-M2/M1));
m1s = m1;
m1e = P1e/(Pw*(M2/M1)-P1e*(1-M2/M1));
m2 = 1-m1;
Mavg = (m1/M1+m2/M2)^-1;
rho = Pw/(8.314/Mavg)/ABST;
Sc = 0.62;
rhoe = Pw/(8.314/Mavg)/ABSTA;
rhos = rho;
nyu = Sc*D12;
g = 9.81;
B = (m1s - m1e)/(1 - m1s);
Gr = g*(rhoe-rhos)*L^3/rho/nyu^2;
Ram = Gr*Sc;
Sh_n = 0.14*Ram^(1/3);
Sh_f = Sh_n + 0.38*Re^0.55*Sc^0.33;
gs = rho*D12*Sh_f/L;

% for boelter with consideration of temperature it is
% 0.09738*ABST-22.5756 instead of constant 1.8. The possible
% explanation is that Raimundo's experiment does not cover a high
% temperature range

gogs = (1/exp(drop)*log(1+B))/B;
```

```
    evap = B*gs*gogs;  
  
end
```

B DAQ Arduino Code

```
// Adafruit Unified Sensor — Version: Latest  
#include <Adafruit_Sensor.h>  
  
// DHT sensor library — Version: Latest  
#include <DHT.h>  
#include <DHT_U.h>  
  
// Adafruit MAX31856 library — Version: Latest  
#include <Adafruit_MAX31856.h>  
  
#include <Wire.h>  
#include "SparkFun_Qwiic_Scale_NAU7802_Arduino_Library.h"  
  
#include "HX711.h"  
  
#define DOUT 3  
#define CLK 2  
  
HX711 scale;  
  
/*  
 */  
#define DHTPIN 22  
#define DHTPIN_2 23  
#define DHTTYPE DHT22 // DHT 22 (AM2302)  
DHT_Unified dht1(DHTPIN, DHTTYPE);  
DHT_Unified dht2(DHTPIN_2, DHTTYPE);  
// All thermocouple breakout boards share these pins  
#define SCK 47  
#define SDO 49  
#define SDI 51  
  
#define CS1 53  
#define CS2 33
```

```

#define CS3 31
#define CS4 29

// // Use software SPI: CS, DI, DO, CLK
Adafruit_MAX31856 thermol = Adafruit_MAX31856(CS1, SDI, SDO, SCK);
Adafruit_MAX31856 thermo2 = Adafruit_MAX31856(CS2, SDI, SDO, SCK);
Adafruit_MAX31856 thermo3 = Adafruit_MAX31856(CS3, SDI, SDO, SCK);
Adafruit_MAX31856 thermo4 = Adafruit_MAX31856(CS4, SDI, SDO, SCK);

Adafruit_MAX31856 thermos[] = {thermol, thermo2, thermo3, thermo4};

void setup() {
    Serial.begin(9600);
    while (!Serial) delay(10);

    dht1.begin();
    dht2.begin();

    for (unsigned int i = 0; i < 4; ++i) {
        thermos[i].begin();
        thermos[i].setThermocoupleType(MAX31856_TCTYPE_T);
    }

    scale.begin(DOUT, CLK);
    scale.set_scale();
    scale.tare(); //Reset the scale to 0

    long zero_factor = scale.read_average(); //Get a baseline reading
}

void loop() {
    unsigned long curr_time = millis();
    Serial.print("Time: " + String(curr_time) + ", ");

    sensors_event_t event;
    dht1.temperature().getEvent(&event);
}

```

```

if (isnan(event.temperature)) {
    Serial.print(F("Error_reading_temperature!"));
} else {
    Serial.print("DHT1_Temp:，“ + String(event.temperature) + ”,“);
}

dht1.humidity().getEvent(&event);
if (isnan(event.relative_humidity)) {
    Serial.print(F("Error_reading_humidity!"));
} else {
    Serial.print("DHT1_Humidity:，“ + String(event.relative_humidity) + ”,“);
    ;
}
}

sensors_event_t event2;
dht2.temperature().getEvent(&event2);
if (isnan(event2.temperature)) {
    Serial.print(F("Error_reading_temperature!"));
} else {
    Serial.print("DHT2_Temp:，“ + String(event2.temperature) + ”,“);
}
}

dht2.humidity().getEvent(&event2);
if (isnan(event2.relative_humidity)) {
    Serial.print(F("Error_reading_humidity!"));
} else {
    Serial.print("DHT2_Humidity:，“ + String(event2.relative_humidity) + ”,“);
    ;
}
}

for (unsigned int i = 0; i < 4; ++i) {
    float temp = thermos[i].readThermocoupleTemperature();
    float cj = thermos[i].readCJTemperature();
    Serial.print("Thermocouple" + String(i) + ":，“ + String(temp) + ”,“);

    uint8_t fault = thermos[i].readFault();
    if (fault) {
        if (fault & MAX31856_FAULT_CJRANGE) Serial.print("Cold_Junction_Range_Fault");
        if (fault & MAX31856_FAULT_TCRANGE) Serial.print("Thermocouple_Range_Fault");
    }
}

```

```

    if (fault & MAX31856FAULT_CJHIGH) Serial.print("Cold_Junction_High_
        Fault");
    if (fault & MAX31856FAULT_CJLOW) Serial.print("Cold_Junction_Low_
        Fault");
    if (fault & MAX31856FAULT_TCHIGH) Serial.print("Thermocouple_High_
        Fault");
    if (fault & MAX31856FAULT_TCLOW) Serial.print("Thermocouple_Low_
        Fault");
    if (fault & MAX31856FAULT_OVUV) Serial.print("Over/Under_Voltage_
        Fault");
    if (fault & MAX31856FAULT_OPEN) Serial.print("Thermocouple_Open_
        Fault");
}
}

Serial.print("Weight: ");
Serial.print(scale.read_average() * 0.002199086165929 - 15.040581847565278, 1)
;
Serial.println();

}

```

References

- [1] M. T. Pauken, “An experimental investigation of combined turbulent free and forced evaporation,” *Experimental Thermal and Fluid Science*,, 1998. [Online]. Available: [https://doi.org/10.1016/S0894-1777\(98\)10038-9](https://doi.org/10.1016/S0894-1777(98)10038-9)
- [2] C. C. Smith, G. Löf, and R. Jones, “Measurement and analysis of evaporation from an inactive outdoor swimming pool,” *Solar Energy*, vol. 53, no. 1, pp. 3 – 7, 1994. [Online]. Available: <http://www.sciencedirect.com/science/article/pii/S0038092X94905975>
- [3] A. M. Raimundo, A. R. Gaspara, A. V. M. Oliveira, and D. A. Quintela, “Wind tunnel measurements and numerical simulations of water evaporation in forced convection airflow,” *International Journal of Thermal Sciences*, vol. 86, no. 1, pp. 28–40, 2014.
- [4] B. R. Hugo and R. P. Omberg, “Evaluation of the fukushima daiichi unit 4 spent fuel pool,” *Int Nucl Saf J*, vol. 4, no. 2, pp. 1–5, 2015, cited By :3. [Online]. Available: www.scopus.com
- [5] M. Shah, “Methods for calculation of evaporation from swimming pools and other water surfaces,” *ASHRAE Transactions*, vol. 120, pp. 3–17, 01 2014.
- [6] M. Q. Brewster, “Evaporation of water at high mass-transfer rates by natural convection air flow with application to spent-fuel pools,” *International Journal of Heat and Mass Transfer*, 2017. [Online]. Available: <https://www.journals.elsevier.com/international-journal-of-heat-and-mass-transfer>
- [7] ——, “Water evaporation and condensation in air with radiation: The self-similar spalding model,” *Journal of Heat Transfer*, 2017. [Online]. Available: <https://doi.org/10.1115/1.4036075>
- [8] L. M. K. Boelter, H. S. Gordon, and J. R. Griffin, “Free evaporation into air of water from a free horizontal quiet surface,” *Industrial & Engineering Chemistry*, vol. 38, no. 6, pp. 596–600, 1946. [Online]. Available: <https://doi.org/10.1021/ie50438a018>